



GAS DAMPER SEAL TEST RESULTS, THEORETICAL CORRELATION, AND APPLICATIONS IN DESIGN OF HIGH-PRESSURE COMPRESSORS

by

Jiming Li

Development Engineer

Frank Kushner

Senior Consulting Engineer

and

Pranabesh DeChoudhury

Senior Consulting Engineer

Elliott Company

Jeannette, Pennsylvania



Jiming Li is a Development Engineer of Advanced Technology at Elliott Company, in Jeannette, Pennsylvania. He has been with Elliott since 1998 and has responsibility for rotor/bearing/seal system dynamics, torsional vibration analysis, development and application of advanced bearings, and damper seals in turbomachinery. Dr. Li has previous experience of more than seven years with rotor-dynamics test and computer program

development, vibration monitoring, vibration data analysis, and troubleshooting of rotating machinery at Zhengzhou Institute of Technology. He has written several technical papers for ASME journals and is a member of ASME.

Dr. Li has a BSME degree from Zhengzhou Institute of Technology (1982), and MSME (1995) and Ph.D. (1999) degrees (Mechanical Engineering) from Texas A&M University.



Pranabesh DeChoudhury has worked for Elliott Company, in Jeannette, Pennsylvania, for the past 29 years in the area of rotor bearing system dynamics. In his current position as Senior Consulting Engineer, his responsibilities include rotor bearing dynamics, bearing design and analysis, torsional dynamics, blade vibration analysis, and troubleshooting field vibration problems.

Dr. DeChoudhury obtained a BSME degree from Jadavpur University (1963), an MSME degree from Bucknell University, and a Ph.D. degree (Mechanical Engineering) from the University of Virginia (1971). He has written several technical papers and has been awarded a patent. He is a registered Professional Engineer in the State of Pennsylvania and is a member of ASME and STLE.



Frank Kushner is a Senior Consulting Engineer for dynamics and acoustics testing/data analysis at Elliott Company, in Jeannette, Pennsylvania. He has 31 years' experience with industrial turbomachinery, with previous experience of four years with the combustion section development group at Pratt and Whitney Aircraft. He was an author for the Ninth and the Twenty-Fifth Turbomachinery Symposiums, as well as for ASME.

Mr. Kushner has a BSME degree from Indiana Institute of Technology (1965) and an MSME degree from Rensselaer Polytechnic Institute (1968). He is a registered Professional Engineer in the State of Pennsylvania and a member of ASME and the Vibration Institute. Mr. Kushner has patents on a blade damping mechanism and for a method to prevent compressor rotating stall.

ABSTRACT

The rotordynamic and leaking characteristics of two types of gas damper seals, honeycomb seal and pocket damper seal, were experimentally evaluated on a rotating test rig. The effect of supply pressure, preswirl, and seal eccentricity on seal dynamic performance was investigated in the tests. The pressurized working gas flowed through the seal and exhausted to atmospheric conditions. The maximum seal supply pressure was limited to 500 psia. By simulating the rotor experimental unbalance response and amplification factors based on a well established rotor model, the equivalent stiffness and damping coefficients were estimated for tested gas damper seals. Experimental results confirm that both honeycomb and pocket damper seals provide high positive effective damping. On the other hand, the pocket damper seal reduces the rotor first critical speed, while the honeycomb seal increases the first critical speed. A correlation study was performed between the identified rotordynamic coefficients and predictions obtained from existing theoretical models for both honeycomb and pocket damper seals. In this paper is discussed as well a damper seal design and its impact on the rotordynamic performance of an industrial high-pressure compressor rotor.

INTRODUCTION

Traditional hydrodynamic instability problems in turbomachinery have been fewer with the extensive applications of tilting-pad bearings that provide greater rotordynamic stability margins. But manufacturers and users found that the stability margins reduced drastically when the design and performance requirements were pushed higher. Since 1980, a number of researches and field investigations have been conducted to recognize the instability mechanisms and resolve vibration problems in high performance turbomachinery. Today, it is realized that in rotating machines with high power densities, fluid forces originating from the balance piston, seals, and impellers or blades can result in unstable operation.

Pioneering research work of Childs, et al. (1989), and Vance and Schultz (1993), has significantly promoted the use of advanced gas damper technologies, honeycomb and pocket damper seals. The rough surface of the honeycomb seal provides higher resistance to the leakage flow in the gap between the sealing land and the rotating surface. Although honeycomb seals were used in the aerospace industry earlier, aerospace honeycomb seals (in aircraft engines) commonly have the teeth-on-rotor/honeycomb-stator configuration for reducing seal leakage. Childs, et al. (1989), experimentally demonstrated that the rotordynamic characteristics of the honeycomb seal in smooth-rotor/honeycomb-stator configuration are superior to the labyrinth seals and annular seals. Many case studies reported recently address the applications of smooth-rotor/honeycomb-stator seals in process-gas compressors and utility steam turbines for eliminating rotordynamic instability problems (Zeidan, et al., 1993; Armstrong and Perricone, 1996). Therefore, the honeycomb seal tested in this paper belongs in the smooth-rotor/honeycomb-stator category. A pocket damper seal was invented and investigated at Texas A&M University around 1990. The pocket damper seal is a new type of modified labyrinth seal that provides a remarkable amount of damping. The pocket damper seal has two unique features, diverging clearance cavities and circumferential damper pockets. The damper pockets are formed by installing partition walls in the annular cavities of the seal. The partition walls also effectively retard the gas swirl that produces the destabilizing cross-coupling force in the seal. Richards, et al. (1995), reported successful applications of pocket damper seals to eliminate subsynchronous vibration in back-to-back industrial compressors.

A series of measurements made at Texas A&M University on honeycomb and pocket damper seals provide important seal rotordynamic force coefficients. However, it seems that the published test data related to both types of damper seal are very limited. Much effort has been made recently to advance theoretical models and computer programs for honeycomb and pocket damper seals (Kleynhans and Childs, 1997; Li, et al., 1999). It is obvious that more experiments are needed to cross-check the existing models and programs. The authors present a test program that was dedicated to honeycomb and pocket damper seal investigations. One of the major objectives of the research was to validate the existing models and computer codes. A reliable correlation study between theoretical predictions and measurements was performed toward providing a guideline in practical designs of the honeycomb seal and the pocket damper seal.

In the design case study of damper seals presented herein, a 14-teeth pocket damper seal was optimized for stabilizing a gas reinjection compressor in the design phase. Aero-logarithmic decrement (aero-log-dec) calculation showed the high-pressure compressor to be highly unstable with standard bearings and impellers and rotating components selected originally. After optimizing the rotating components and tilting-pad journal bearings, the predicted minimum aero-log-dec was still not acceptable. Various bearing configurations examined could not achieve a satisfactory result. The conventional center seal in this high-pressure back-to-back compressor would provide substantial

destabilizing force. Therefore, a damper seal was proposed to be installed to provide necessary positive damping and reduce cross-coupled stiffness to result in a stable rotor-bearing-seal system.

The university referred to in this paper is Texas A&M University and the university research laboratory referred to is the Turbomachinery Laboratory at Texas A&M University.

TEST APPARATUS AND PROCEDURE

Test Rig

A cross-section of the gas seal test stand is shown in Figure 1. A 50 hp variable-speed, induction motor drives the test rotor through a flexible coupling. The nominal shaft diameter of the flexible rotor is 3.875 inches. The rotor has two rotating disks with 9.75 inch OD and is supported by two ball bearings located 44 inches apart. On each rotating disk, there are tapped holes for final balancing the rotor and adding intentional unbalance masses in tests with seals. The design first critical speed of the flexible rotor is 6600 rpm. Use of ball bearings instead of hydrodynamic bearings is to assure low damping for more accurate evaluation of seal properties.

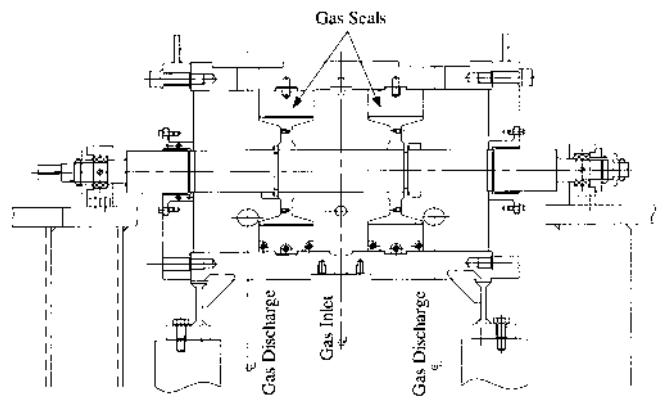


Figure 1. Cross-Section of Gas Seal Test Stand.

As shown in Figure 1, there are two identical test gas damper seals installed back-to-back in the horizontally split casing. Casing supports are separate from those for the bearings to give the ability to easily offset the seals radially. Ball bearings are double-row angular contact design, using ISO series 10 matched pairs, lubricated with grease rated to 230°F. The coupling end bearing has fixed inner and outer retainers, while the outboard bearing uses a wave spring to compensate for relative thermal growths. The test stand is supplied with nitrogen gas from a high-pressure tanker, fitted with a high flow valve. The inlet pressure is set to the desired value through an electronically controlled upstream valve providing flow to the central plenum chamber between the two test gas seals. Thus axial thrust loads on the bearings are minimized, with two leakage flows going out in opposite directions and exhausting to the atmosphere. The total mass flow rate is measured with a calibrated orifice. The upstream and downstream gas temperatures and the temperatures of the ball bearing outer retainers are measured as well. Both static and total pressures at the seal entrance are measured besides the pressures at casing inlet and outlet. At the internal inlet walls, holes are available to install 90 degree spray nozzles to somewhat increase the inherent tangential swirl at seal entrances.

Test Gas Damper Seals

Two 9.75 inch diameter by 5.25 inch long, pocket damper seals were first tested on the test stand with the flexible rotor. The effective sealing length of the pocket damper seal is 4.25 inches. The test pocket damper seal has 10 teeth and a minimum seal radial clearance of 10 mils. Therefore, there are five damper cavities

separated by four inactive annular cavities shown in Figure 2. For each damper cavity, the ratio of the exit clearance C_{exit} to the inlet clearance C_{inlet} is equal to 1.8. Based on the pocket damper seal theory, the longer the damper cavity pitch is, the more damping the seal generates. The damper cavity pitch is 2.5 times the pitch of the inactive cavity for the test pocket damper seals. The cavity depth is 0.50 inches and seal teeth thickness is 0.125 inches. For comparison, two honeycomb seals with the same dimension were tested on the test stand with the same flexible rotor. The test honeycomb seal has a straight through radial clearance of 10 mils, equal to the minimum radial clearance of the pocket damper seal. As shown in Figure 3, the effective cell land of the honeycomb seal is 4.293 inches. The honeycomb cell dimensions are 0.09 inch depth and 0.062 inch width.

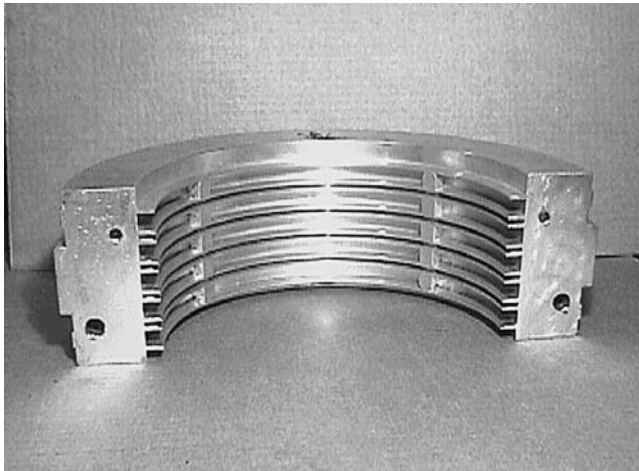


Figure 2. Pocket Gas Damper Seal.

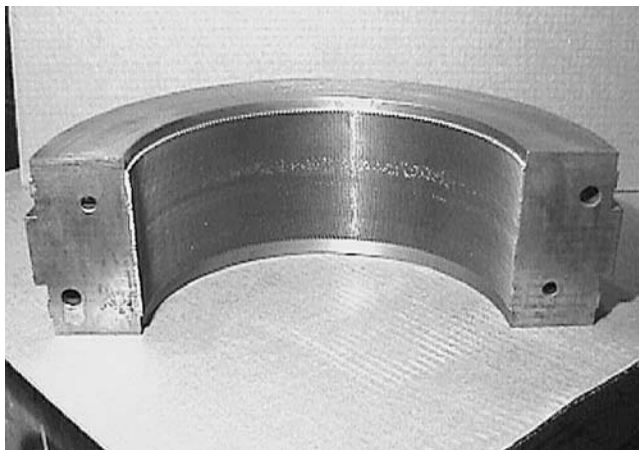


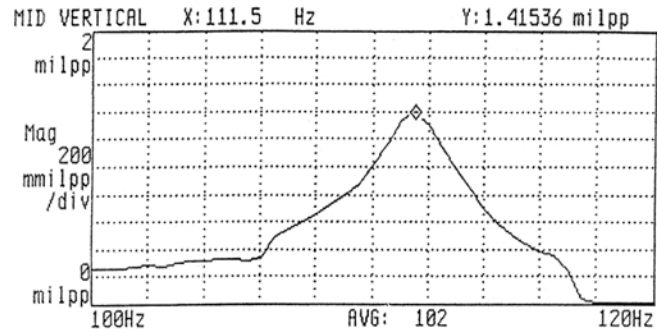
Figure 3. Honeycomb Seal.

Test Procedure

Since the temperature of the working gas is lower than the ambient temperature, in each test the rotor first runs at 500 rpm about 30 minutes normally with an inlet pressure of 3 psig, which keeps the gas coming through the path between the seal and rotating disk surfaces. When the system reaches its equilibrium point, the rotor is brought to a speed somewhat below the critical speed and the inlet valve is adjusted to maintain gas pressure at a specified test pressure. Then, the rotor is driven by the motor to pass through its first critical speed region to full speed, with a controlled coastdown using internal motor braking, while the rotor unbalance responses are

measured at the shaft midspan and both shaft ends. Consequently, experimental rotor critical speeds and amplification factors are identified from the measured rotor unbalance response plots. Maximum seal inlet pressures were limited to 500 psia for one build, and then to 235 psia for the pocket damper seal and the honeycomb seal, respectively. No higher supply pressures were tested since the extremely high damping from both pocket seal and honeycomb seal was demonstrated at lower seal inlet pressure levels.

With much fine tuning due to low ball bearing damping, the flexible rotor was initially balanced to minimize the effect of the residual imbalance such that maximum synchronous response amplitudes measured at both shaft ends were less than 0.80 mil and the response at rotor midspan was less than 2.5 mils. The baseline vibration of the rotor was measured before test damper seals were installed. A typical baseline of the rotor unbalance response to the residual unbalance mass is shown in Figure 4. To excite the unbalance response of the rotor with the first mode in tests, an intentional imbalance mass of 0.51 oz-in was added at the outboard rotating disk. Each pair of tested gas damper seals was tested first at the centered position. Then the seals were tested at an off-centered position. The casing was lifted 5 mils by adding shims between the casing and stand to obtain a 50 percent eccentric ratio of the seal eccentricity to the seal inlet clearance. Two gas injection conditions were investigated in tests, with and without additional swirl from the 90 degree swirl nozzles in the rotor rotating direction. Due to low values of additional swirl at speed, the swirl nozzles were only marginally effective at both centered and off-



centered seal operations.

Figure 4. Vertical Unbalance Response of Flexible Rotor without Gas Damper Seal at Inlet Pressure 14.7 PSIA (Residual Unbalance and Probe at Midspan).

EXPERIMENTAL RESULTS AND COMPARISON TO PREDICTIONS

Pocket Damper Seal Test Results

Typical unbalance responses of the flexible rotor with the pocket damper seals are shown in Figures 5, 6, and 7 at several test seal inlet pressures of 85, 225, and 500 psia, respectively. Note that in Figures 6 and 7, the unbalance responses were obtained with a 0.51 oz-in intentional unbalance on the rotor, whereas the unbalance response in Figure 5 was measured with residual unbalance only. Experimental results confirmed that the pocket damper seal provided high positive damping to suppress rotor vibration. The average amplification factor of unbalance response dramatically decreased with an increase in the seal inlet pressure. The average critical speeds and amplification factors in both vertical and horizontal directions were derived from the rotor unbalance responses measured at both shaft ends and rotor midspan, and presented in Table 1. It was noted that the amplification factor (AF) was very small at 500 psia. A conservative AF of 1.5 was estimated at 500 psia inlet pressure. It is apparent that the negative stiffness of the pocket damper seal reduced the rotor critical speed in tests.

A number of gas seal tests confirmed that a long labyrinth seal has negative stiffness (Childs, 1993). No users report that the machine critical speed location shifts obviously after a pocket damper seal is installed to replace the labyrinth seals. Note that the change in the critical speed and AF was caused by two gas pocket damper seals in this test rig.

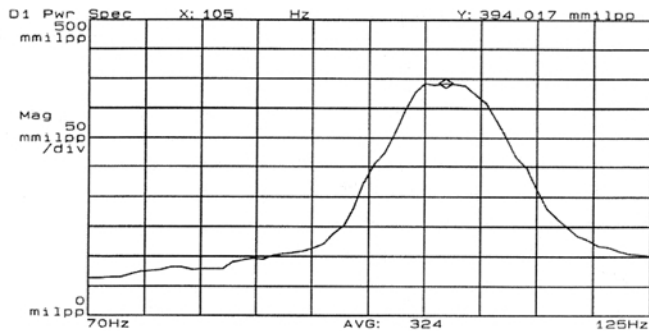


Figure 5. Vertical Unbalance Response of Flexible Rotor with Centered Pocket Damper Seal at Inlet Pressure 85 PSIA (Residual Unbalance and Probe at Midspan).

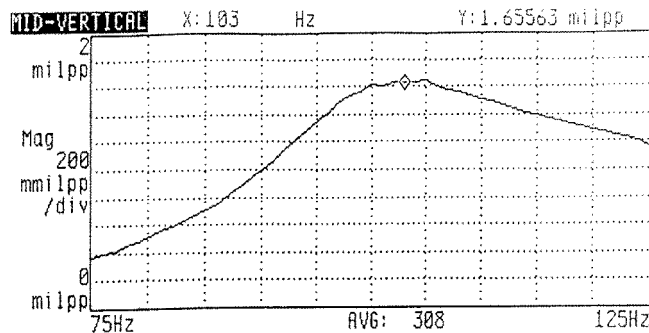


Figure 6. Vertical Unbalance Response of Flexible Rotor with Centered Pocket Damper Seal at Inlet Pressure 225 PSIA (0.51 oz-in Unbalance and Probe at Midspan).

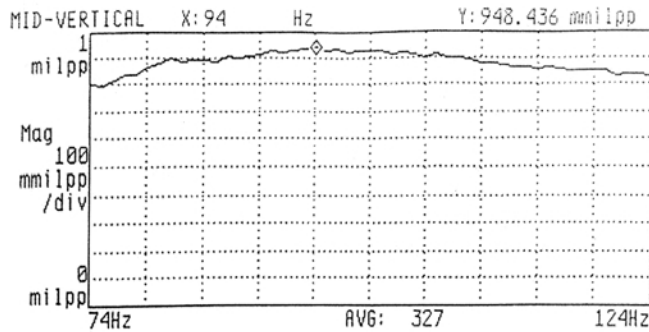


Figure 7. Vertical Unbalance Response of Flexible Rotor with Centered Pocket Damper Seal at Inlet Pressure 500 PSIA (0.51 oz-in Unbalance and Probe at Midspan).

Identified Damping and Stiffness of Pocket Damper Seal

Before evaluating seal force coefficients, a lateral vibration model of the test rotor bearing system was established. A verified rotordynamic program was used to estimate the effective stiffness and damping coefficients of the pocket damper seal at test conditions. In calculations, each test seal was represented by its effective stiffness and damping coefficients, which were added into the rotor bearing system model. The experimental amplification factors and critical speeds of the rotor in Table 1 were reproduced with the program by adjusting seal effective rotordynamic

Table 1. Experimental Critical Speeds and Amplification Factors of Flexible Rotor on Gas Seal Test Stand/Pocket Damper Seal (9.75 inches × 5.25 inches).

Test Conditions	Vertical		Horizontal	
	Critical Speed	AF	Critical Speed	AF
Baseline w/o seal Inlet P = 14.7 psia	6690 rpm	40.3	6360 rpm	84.0
Centered seal Inlet P = 85 psia Intentional pre-swirl	6420 rpm	8.39	6060 rpm	8.24
Centered seal Inlet P = 215 psia Intentional pre-swirl	6000 rpm	3.83	5800 rpm	3.92
Centered seal Inlet P = 225 psia No intentional pre-swirl	6180 rpm	3.16	6000 rpm	3.30
Centered seal Inlet P = 500 psia No intentional pre-swirl	5640 rpm	<1.5	5640 rpm	<1.5
Off-centered seal Inlet P = 225 psia Intentional pre-swirl	5850 rpm	4.32	5580 rpm	3.74

coefficients carefully. Note that the seal force coefficients at 500 psia were obtained with an AF of 1.5. The effective damping and stiffness coefficients of the pocket damper seal are identified at all test conditions and summarized in Table 2. It is clear that pocket damper seal has negative stiffness, which resulted in a drop in the rotor critical speed. The magnitudes of damping and stiffness of the pocket damper seal increased dramatically with increasing seal supply pressure. The effect of seal eccentricity and gas preswirl was not well identified due to a lack of test points for the pocket damper seal. Based on the limited test data, it seems that both gas preswirl and seal eccentricity decrease the effective damping and increase the magnitude of the effective stiffness for pocket damper seals.

Table 2. Identified Seal Effective Damping and Stiffness Coefficients from Measured Unbalance Responses of Flexible Rotor/Pocket Damper Seal (9.75 inches × 5.25 inches).

Test Conditions	Vertical		Horizontal	
	Stiffness (lb/in)	Damping (lb-s/in)	Stiffness (lb/in)	Damping (lb-s/in)
Centered seal Inlet P = 85 psia Intentional pre-swirl	- 6,300	12.2	- 9,300	13.2
Centered seal Inlet P = 215 psia Intentional pre-swirl	- 19,000	22.0	- 18,000	24.0
Centered seal Inlet P = 225 psia No intentional pre-swirl	- 15,000	30.0	- 11,000	30.0
Centered seal Inlet P = 500 psia No intentional pre-swirl	- 55,000	81.0	- 48,000	85.0
Off-centered seal Inlet P = 225 psia Intentional pre-swirl	- 23,300	20.0	- 23,200	21.6

Comparison to Theoretical Predictions for Pocket Damper Seal

Theoretical model development for the design of the pocket damper seal is still inadequate when compared to the experimental

investigations and industrial applications. One state-of-the-art model and computer program for pocket damper seal analysis was developed and updated by Dr. John Vance of the university research laboratory. The model only accounts for axial flow through the seal while neglecting circumferential swirl flow in the seal. Therefore only direct seal rotordynamic coefficients K and C can be predicted. Another limitation is that the program can only handle the centered pocket damper seal cases. The model has been used for predictions in several industrial applications of pocket damper seals (Richard, et al., 1995). The same program was adopted in this research to calculate the leakage and rotordynamic coefficients of the test pocket damper seal.

The damping and stiffness coefficients of the pocket damper seal at test conditions are calculated and shown in Tables 3 and 4. The identified seal coefficients in the tables are the average values in the vertical and horizontal directions. Comparisons validate the existing model to be acceptable for general designs of pocket damper seals. The model predicts the trend of seal damping versus supply pressure properly, while underpredicting the effective damping coefficients 30 to 55 percent in the test pressure range. The existing program correctly predicts the stiffness of the pocket damper seal to be negative. Except at 225 psia, the deviation of predicted seal stiffness coefficient is within ± 11 percent of experimental results. Note that the magnitude of pocket damper seal stiffness is considerably small when compared to typical compressor shaft stiffness and journal bearing stiffness. The seal leakage rates are also evaluated with the program and given in Table 5 with the measured leakage data for the test pocket damper with a minimum 10 mils seal radial clearance. The measurements show that the influence of gas preswirl and seal eccentricity on seal leakage is negligible for the pocket damper seal. The comparison shows that the analytical model underpredicts seal leakage around 14 to 20 percent in the pressure range tested. Note that the predicted leakage flow is choked at the last seal blade at all test seal supply pressures.

Table 3. Comparison of Predicted Damping to Identified Average Damping of Pocket Damper Seal with Flexible Rotor.

Test Conditions	Identified Damping (lb-s/in)	Predicted Damping (lb-s/in)	Relative Error
Centered seal Inlet P = 85 psia Intentional pre-swirl	12.7	6.33	- 50.2%
Centered seal Inlet P = 215 psia Intentional pre-swirl	23.0	16.0	- 30.4%
Centered seal Inlet P = 225 psia No intentional pre-swirl	30.0	16.7	- 44.3 %
Centered seal Inlet P = 500 psia No intentional pre-swirl	83.0	38.1	- 54.1%

Honeycomb Seal Test Results

Measurements demonstrated that the honeycomb seal, similar to the pocket damper seal, provided high effective damping. The measured amplification factors significantly decreased with the seal inlet pressure. In contrast to the pocket damper seal, the test honeycomb seal resulted in a substantial increase in the rotor first critical speed. Consequently, the test speed range was extended up to 12,000 rpm in honeycomb seal tests. Typical unbalance responses of the flexible rotor with honeycomb seal are shown in Figures 8, 9, and 10 at the seal inlet pressures equal to 65, 130, and 235 psia, respectively. The maximum seal supply pressure was

Table 4. Comparison of Predicted Stiffness to Identified Average Stiffness of Pocket Damper Seal with Flexible Rotor.

Test Conditions	Identified Stiffness (lb/in)	Predicted Stiffness (lb/in)	Relative Error
Centered seal Inlet P = 85 psia Intentional pre-swirl	- 8,700	- 8,100	- 6.9%
Centered seal Inlet P = 215 psia Intentional pre-swirl	- 18,500	- 20,500	10.8%
Centered seal Inlet P = 225 psia No intentional pre-swirl	- 13,000	- 21,300	63.8%
Centered seal Inlet P = 500 psia No intentional pre-swirl	- 51,500	- 48,700	- 5.7%

Table 5. Comparison of Predicted Leakage Rate to Measured Leakage Rate of Pocket Damper Seal with Flexible Rotor.

Test Conditions	Measured Leakage (lbs/min)	Predicted Leakage (lbs/min)	Relative Error
Centered seal Inlet P = 85 psia Intentional pre-swirl	17.5	15.1	- 13.7%
Centered seal Inlet P = 215 psia Intentional pre-swirl	48.5	38.3	- 21%
Centered seal Inlet P = 225 psia No intentional pre-swirl	49.5	40.1	- 19%
Centered seal Inlet P = 500 psia No intentional pre-swirl	111.5	89.1	- 20%
Off-centered seal Inlet P = 225 psia Intentional pre-swirl	50.0		

limited to 235 psia for the honeycomb seal. It became difficult to identify the critical speed and amplification factor from the measured unbalance responses at higher supply pressures. The average measured critical speeds and amplification factors were derived from the rotor unbalance responses at both shaft ends and rotor midspan, and are presented in Table 6. Three conservative amplification factors of 2.50, 2.35, and 2.68 were approximately estimated when the seal supply pressure was equal to or above 230 psia. Note that the changes in the measured critical and AF of the flexible rotor resulted from two gas honeycomb damper seals in this test rig.

Identified Effective Damping and Stiffness of Honeycomb Seal

To evaluate the honeycomb seal rotordynamic coefficients, each test honeycomb seal was simplified as its effective stiffness and damping coefficients were added into the rotor/bearing/seal system model. Note that the effective damping of the honeycomb seal takes into account the combined rotordynamic influence from the direct damping and the cross-coupled stiffness. Memmott (1999) reported that the cross-coupled stiffness of a honeycomb seal is substantial though the honeycomb seal has much higher damping

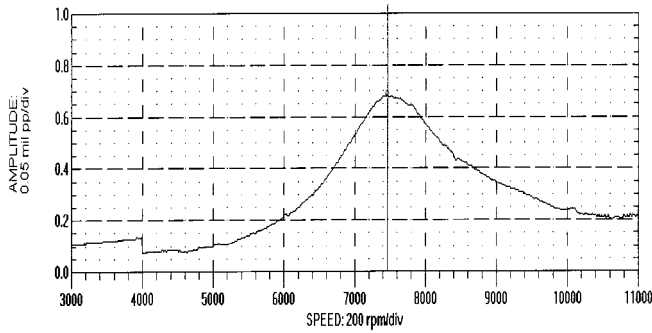


Figure 8. Vertical Unbalance Response of Flexible Rotor with Off-Centered Honeycomb Seal at Inlet Pressure 65 PSIA (0.51 oz-in Unbalance and Probe at Outboard End).

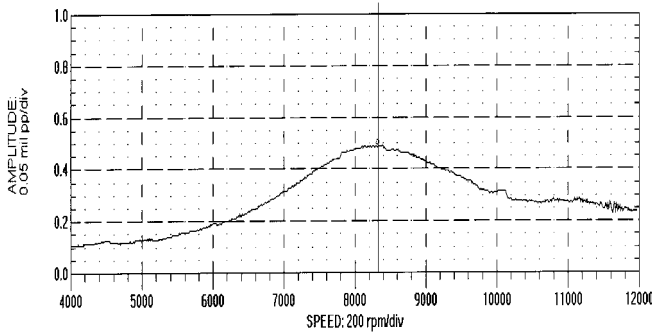


Figure 9. Vertical Unbalance Response of Flexible Rotor with Off-Centered Honeycomb Seal at Inlet Pressure 130 PSIA (0.51 oz-in Unbalance and Probe at Outboard End).

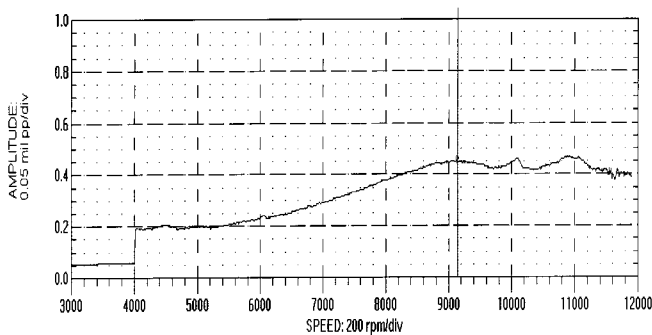


Figure 10. Vertical Unbalance Response of Flexible Rotor with Off-Centered Honeycomb Seal at Inlet Pressure 235 PSIA (0.51 oz-in Unbalance and Probe at Outboard End).

than labyrinth seals. Using the same rotordynamic program to simulate the measured amplification factors and critical speeds shown in Table 6, the effective damping and stiffness coefficients of the honeycomb seal are identified and presented in Table 7. It is clear that honeycomb seals provide positive effective stiffness and positive damping. The magnitudes of damping and stiffness of honeycomb seals increase with increasing seal supply pressure. The stiffness coefficients are sensitive to the seal eccentricity. Compared to the centered honeycomb seal, the off-centered honeycomb seal has smaller effective stiffness and damping. Induced gas preswirl always reduces the seal effective damping. In most cases, gas preswirl at seal entrance increases the effective stiffness for an off-centered operation.

A comparison between Tables 2 and 7 shows that the honeycomb seal provides more effective damping than the pocket damper seal at similar test conditions. The honeycomb seal has positive effective stiffness while the pocket damper seal has negative effective stiffness. Note that the gas preswirl was

Table 6. Experimental Critical Speeds and Amplification Factors of Flexible Rotor on Gas Seal Test Stand/Honeycomb Seal (9.75 inches \times 5.25 inches).

Test Conditions	Vertical critical speed / AF	Horizontal critical speed / AF
Baseline w/o seal Inlet P = 14.7 psia	6690 rpm / 40.3	6360 rpm / 84.0
Centered seal Inlet P = 90 psia No intentional pre-swirl	7800 rpm / 4.85	7310 rpm / 4.84
Centered seal Inlet P = 235 psia No intentional pre-swirl	9780 rpm < 2.50	9430 rpm < 2.50
Off-centered seal Inlet P = 65 psia No intentional pre-swirl	7460 rpm / 5.31	7060 rpm / 6.79
Off-centered seal Inlet P = 65 psia Intentional pre-swirl	7425 rpm / 5.44	7030 rpm / 7.48
Off-centered seal Inlet P = 130 psia No intentional pre-swirl	8315 rpm / 3.35	7845 rpm / 4.28
Off-centered seal Inlet P = 130 psia Intentional pre-swirl	8485 rpm / 3.58	7860 rpm / 4.55
Off-centered seal Inlet P = 235 psia No intentional pre-swirl	9130 rpm < 2.35	8460 rpm < 2.35
Off-centered seal Inlet P = 230 psia Intentional pre-swirl	9310 rpm < 2.68	8605 rpm < 2.68

Table 7. Identified Seal Effective Damping and Stiffness Coefficients from Measured Unbalance Responses of Flexible Rotor/Honeycomb Seal (9.75 inches \times 5.25 inches).

Test Conditions	Vertical		Horizontal	
	Stiffness (lb/in)	Damping (lb-s/in)	Stiffness (lb/in)	Damping (lb-s/in)
Centered seal Inlet P = 90 psia No intentional pre-swirl	36,000	36.9	28,000	27.0
Centered seal Inlet P = 235 psia No intentional pre-swirl	96,000	87.0	93,000	85.0
Off-centered seal Inlet P = 65 psia No intentional pre-swirl	24,500	29.0	20,000	20.0
Off-centered seal Inlet P = 65 psia Intentional pre-swirl	24,000	26.0	20,000	19.0
Off-centered seal Inlet P = 130 psia No intentional pre-swirl	49,100	61.0	45,500	36.4
Off-centered seal Inlet P = 130 psia Intentional pre-swirl	54,000	57.4	46,000	34.7
Off-centered seal Inlet P = 235 psia No intentional pre-swirl	71,000	85.0	55,000	74.0
Off-centered seal Inlet P = 230 psia Intentional pre-swirl	80,000	78.0	65,000	69.0

relatively low in the tests for both honeycomb and pocket damper seals. It is estimated that the gas preswirl ratios were less than 0.5 even in the cases in which the intentional gas swirl was induced by the angled inlet gas nozzles. The superior damping performance of honeycomb seals herein cannot be simply extended to other conditions untested, especially for high gas preswirl cases. Analyses and experiments show that the partition walls in the grooves of pocket damper seals retard the development of circumferential flow in the pocket seals significantly (Li, et al., 1999).

Comparison to Theoretical Predictions for Honeycomb Seal

In this investigation, one updated analytical tool is available from Dr. Dara Childs of the university research laboratory. The program was developed based on an isothermal, two-control-volume, bulk-flow model for a honeycomb seal analysis (Kleynhans and Childs, 1997). Only synchronous rotordynamic coefficients of the test honeycomb seal are reported in this presentation though the code can predict seal nonsynchronous rotordynamic coefficients as well. Currently the updated computer program can only calculate the rotordynamic coefficient of a centered honeycomb seal. Theoretically the program gives all eight rotordynamic coefficients. For a centered seal, it assumes that the direct stiffness and damping coefficients are symmetric ($K_{xx} = K_{yy}$, $C_{xx} = C_{yy}$), and the cross-coupled stiffness and damping coefficients are skew-symmetric ($K_{xy} = -K_{yx}$, $C_{xy} = -C_{yx}$). In practice, it is not uncommon to neglect the cross-coupled damping coefficients (C_{xy} , C_{yx}) for gas seals. Therefore, the predicted effective stiffness and damping (synchronous coefficients) of the honeycomb seal are derived from the following formulas:

$$K_{ef} = K_{xx} \quad (1)$$

$$C_{ef} = C_{xx} \left(1 - \frac{K_{xy}}{\Omega C_{xx}} \right) \quad (2)$$

where:

Ω (rad/s) is the rotating angular velocity of the rotor.

It is seen that the predicted effective damping coefficient accounts for both the cross-coupled stiffness and the direct damping for honeycomb seals. Any factors that promote the cross-coupled stiffness, such as gas preswirl, would reduce the seal effective damping.

The effective damping and stiffness coefficients of the centered honeycomb seal are calculated at the measured critical speeds. Both the identified and predicted coefficients in Tables 8 and 9 are the average values of the effective seal coefficients in the vertical and horizontal directions. The program predicts the effective damping well at low pressure, while it underpredicts the effective damping coefficients 32 percent at the high seal inlet pressure of 235 psia. The program correctly predicts honeycomb seal stiffness to be positive. In the test pressure range, the code consistently underpredicts the stiffness coefficients about 15 percent. The research work confirms that the predicted honeycomb seal coefficients are acceptable in designs when the pressure drop is in the range tested. Further correlation work between experiments and predictions at larger differential pressures across the seal and higher gas preswirl ratios is suggested.

A comparison of seal leakage rates is presented in Table 10 for the test honeycomb seal with a 10 mil seal radial clearance. The values in the table are equal to one-half of the total measured mass flow rate since there are two identical seals installed in the casing. The comparison shows that the analytical program overpredicts seal leakage around 20 percent in the pressure range tested. Note that the predicted leakage flow is choked at the seal exit for all test seal supply pressures. Although the test data from off-centered honeycomb seals are not reported in Table 10, the measurements

Table 8. Comparison of Predicted Effective Damping to Identified Average Damping of Honeycomb Seal with Flexible Rotor:

Test Conditions	Identified Damping (lb-s/in)	Predicted Damping (lb-s/in)	Relative Error
Centered seal Inlet P = 90 psia No intentional pre-swirl	32.0	32.3	1.0%
Centered seal Inlet P = 235 psia No intentional pre-swirl	86.0	58.4	- 32.1%

Table 9. Comparison of Predicted Effective Stiffness to Identified Average Stiffness of Honeycomb Seal with Flexible Rotor:

Test Conditions	Identified Stiffness (lb/in)	Predicted Stiffness (lb/in)	Relative Error
Centered seal Inlet P = 90 psia No intentional pre-swirl	32,000	27,200	- 15%
Centered seal Inlet P = 235 psia No intentional pre-swirl	94,500	82,400	-12.8%

illustrate that leakage rate slightly increases with the seal eccentricity while the effect of gas preswirl on seal leakage is negligible. A comparison between Tables 5 and 10 shows that the leakage rate of pocket damper seals is roughly twice that of honeycomb seals with the same minimum seal clearance.

Table 10. Comparison of Predicted Leakage Rate to Measured Leakage Rate of Honeycomb Seal with Flexible Rotor:

Test Conditions	Measured Leakage (lbs/min)	Predicted Leakage (lbs/min)	Relative Error
Centered seal Inlet P = 90 psia No intentional pre-swirl	9.4	11.5	22.3%
Centered seal Inlet P = 235 psia No intentional pre-swirl	26.2	31.5	20.2%

A CASE STUDY OF POCKET DAMPER SEAL DESIGN

Stability Problem in a Compressor Rotor

The example discussed hereinafter arises from a rotordynamic analysis of a preliminary design-phase centrifugal compressor for natural gas reinjection service. This designed back-to-back compressor has a total of five stages and the design maximum continuous speed is 14,366 rpm. The molecular weight of working gas is 19.7 and the average gas density is 14.37 lb/ft³. The discharge pressure and temperature are 7280 psia and 252°F, respectively. The differential pressure across the center labyrinth seal is 2515 psi. The preselected center seal is a 7.50 inch long interlocked labyrinth seal shown in Figure 11. The compressor rotor is supported by two five-shoe tilting-pad journal bearings.

The stability of the high-pressure compressor was one of the major concerns from the beginning. The flex-ratio (maximum continuous speed/first rigid support critical speed) of the initial rotor was 1.97, and the minimum aero-log-dec of the rotor was less than -0.50 at the rated operating conditions. For a more rigid rotor,

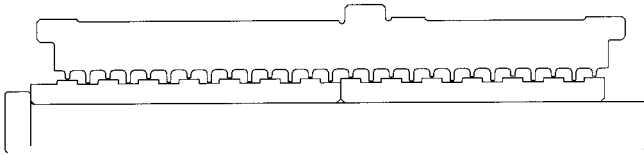


Figure 11. A Schematic of Preselected Center Labyrinth Seal.

a number of actions were taken that included increasing shaft diameter at separation seal and center seal, using light impellers made of titanium, cutting the inlet and discharge spacing, and reducing coupling and gas seal cartridge weights. Finally, the optimized rotor bearing span was 47.58 inches and total rotor weight was 413.5 lb. The rotor flex-ratio was reduced to 1.55 and stability of the rotor was improved. However the minimum aero-log-dec still had a negative value of -0.128 . Aero-log-dec is an acceptable indicator to justify the stability of high-performance turbomachinery for manufacturers and users. Theoretically, a machine is unstable when aero-log-dec is negative, and a positive aero-log-dec indicates the machine to be stable in the rotordynamic point of view. It is common that OEM's and users of turbomachinery have their minimum acceptable aero-log-dec for a particular application based on their experience to keep a sufficient stable margin. For this case, a minimum aero-log-dec of 0.378 was required with the expected aerodynamic force ($Q = 9859$ lb/in) at each impeller. Although the tilting-pad journal bearings have not been optimized in this phase yet, it is realized that to resort to a damper is definitely necessary for stabilizing the compressor. The bearing clearances of the preselected tilting-pad journal bearing with the bearing load between pads configuration are shown in Table 11.

Table 11. Preselected Five-Shoe, Center-Pivot, Tilting-Pad Journal Bearing (3.50 inches \times 1.60 inch).

	Diametral Assembly CLR (inches)	Diametral Pad Machined CLR (inches)	Preload
Maximum Bearing Clearance	0.0055	0.0070	0.214
Minimum Bearing Clearance	0.0035	0.0075	0.533

Pocket Damper Seal Design

A pocket damper seal was proposed to replace the preselected center labyrinth seal. Rotor midspan is a superior position for an external damper to enhance the rotor stability in the first flexible mode. A stability study of the optimized rotor showed that approximately 85 lb-s/in damping is needed to obtain the minimum acceptable aero-log-dec. The overall dimensions of the proposed center pocket damper are 6.25 inches in diameter and 7.50 inches long. The seal inlet radial clearance is 0.012 inch. A damper cavity clearance ratio (C_{exit}/C_{inlet}) of 1.33 was selected. The determination of seal teeth number and pocket depth was based on the predictions in Table 12.

Considering the expected center seal leakage rate to be 373.1 lb/min at guarantee conditions, a pocket damper seal with 14 teeth and 0.25 inch cavity depth was selected. The pocket damper seal would satisfy the leakage requirement and provide 85.9 lb-s/in damping to raise the minimum aero-log-dec to 0.373, which was slightly less than the required value 0.378. Due to using shallow pocket design, the seal teeth thickness could be reduced to 0.06 inch to increase the effective length of damper cavities. Therefore, the damping of the damper seal was increased substantially. The pitch ratio (active cavity pitch/inactive cavity pitch) of the

Table 12. Damping and Leakage of Pocket Damper Seal Versus Teeth Number and Cavity Depth (Seal Radial CLR 0.012 inch and Teeth Thickness 0.125 inch).

Teeth Number	Damping (Lb-s/in)		Leakage (Lb/min)
	Depth 0.25"	Depth 0.50"	
10	174.3	193.7	404.0
12	119.5	131.9	361.6
14	85.9	94.0	329.3
16	63.7	69.2	303.7
18	48.4	52.2	282.7

designed pocket seal is equal to 2.61, similar to the pitch ratio of the test pocket damper seal discussed in this presentation. Predictions showed the change in the teeth thickness has no influence on the seal leakage. A schematic of the final designed 14-teeth, pocket damper seal is shown in Figure 12, and its predicted dynamic characteristics are given in Table 13. A stability analysis of the optimized compressor rotor was conducted with the pocket damper seal and the preselected tilt-pad journal bearings. Corresponding values of the aero-log-dec are presented in Table 14. It is seen that the predicted minimum aero-log-dec 0.545 of the rotor with the pocket damper is well above the criterion value 0.378.

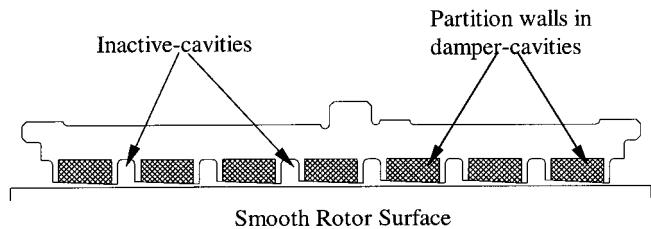


Figure 12. Center Gas Pocket Damper Seal with 14 Teeth.

Table 13. Damping, Stiffness, and Leakage of 14-Teeth Pocket Damper Seal (Seal Radial CLR 0.012 inch, Cavity Depth 0.25 inch, and Teeth Thickness 0.06 inch).

Damping (lb-s/in)	Stiffness (lb/in)	Leakage (lb/min)
115.1	-157,493	329.3

Table 14. Estimated Aero-Log-Dec of the Optimized Rotor with Pocket Damper Seal and Preselected Journal Bearings at Maximum Continuous Speed (14,366 RPM).

	Aero-log-dec with Pocket Damper	Aero-log-dec w/o Pocket Damper	Basic log-dec
Maximum Bearing Clearance	1.028	0.355	0.711
Minimum Bearing Clearance	0.545	-0.128	0.159

Final Solution to Enhance the Compressor Rotor Stability

Besides using a pocket damper seal, a process to optimize the tilting-pad journal bearings was performed as well. A number of bearing configurations were examined to investigate the effect of load direction, pivot location, number of pads, and bearing preload on the rotor stability. Calculations showed that there is very little difference between the rotordynamic performance of the rotor with five-shoe journal bearings and four-pad journal bearings, respectively. The stability analysis further confirmed that a center-pivot, load between pads design was preferred when compared with other off-center-pivot or center-pivot with load on pads configurations. It was noted that the aero-log-dec of the rotor is sensitive to the bearing preload. The optimized bearing parameters are given in Table 15. A comparison to Table 11 shows that the bearing preload is reduced in the optimized bearing design.

Table 15. Optimized Five-Shoe, Centered-Pivot, Tilting-Pad Journal Bearing (3.50 inches × 1.60 inch).

	Diametral Assembly CLR (inches)	Diametral Pad Machined CLR (inches)	Preload
Maximum Bearing Clearance	0.00665	0.0070	0.050
Minimum Bearing Clearance	0.00473	0.0075	0.369

Finally, a combination of the optimized tilt-pad bearings and pocket damper seal was selected to upgrade the stability of the high-pressure compressor rotor. The aero-log-dec values of the rotor were calculated at the maximum continuous speed at 14,366 rpm, and presented in Table 16. The minimum aero-log-dec of the rotor is further raised to 0.824, which is even larger than twice the minimum acceptable aero-log-dec. Since there are some uncertainties in the estimation of the aerodynamic forces at impellers, it is common for manufactures and users to examine the sensitivity of aero-log-dec to the destabilizing forces for a critical machine. Figure 13 shows that the threshold of the aerodynamic force is increased from 12,500 lb/in to 34,000 lb/in with the pocket damper seal at minimum journal bearing clearance case. The predictions illustrate that the aero-log-dec of the rotor is more sensitive to the aerodynamic cross-coupling force with the maximum bearing clearance. When the pocket damper seal is installed, the predicted threshold of destabilizing aerodynamic force at each impeller is increased from 14,500 lb/in to 24,000 lb/in at the maximum bearing clearance case.

Table 16. Estimated Aero-Log-Dec of the Optimized Rotor with Pocket Damper Seal and Optimized Journal Bearings at Maximum Continuous Speed (14,366 RPM).

	Aero-log-dec with Pocket Damper	Aero-log-dec w/o Pocket Damper	Basic log-dec
Maximum Bearing Clearance	1.207	0.472	0.679
Minimum Bearing Clearance	0.824	0.098	0.433

CONCLUSIONS

Test data reduction and theoretical correlation of gas damper seals have been completed on a gas seal test stand for the pocket damper seal and the honeycomb seal, respectively. The seal effective stiffness and damping coefficients were estimated with a rotordynamics program based on the experimental damped critical

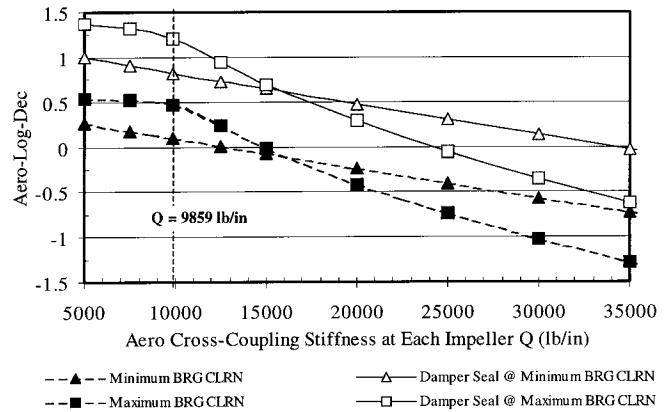


Figure 13. Logarithmic Decrement Sensitivity Due to Aerodynamic Cross-Coupling Stiffness at Each Impeller (14,366 RPM).

speeds and amplification factors of the flexible rotor. Comparisons of seal leakage and dynamic force coefficients were made between the theoretical predictions and the test results. The following conclusions are obtained from this investigation:

- Both pocket damper seal and honeycomb seal provide high positive damping to suppress rotor vibration effectively. At the tested conditions, the honeycomb seal has more effective damping than the pocket damper seal. Induced gas swirl at the seal entrance reduces the effective damping of the test seals. An antiswirl mechanism at the seal entrance is still favorable for maximizing the damping performance of the pocket damper seal and honeycomb seal. Seal eccentricity results in a decrease in seal damping moderately for both honeycomb and pocket damper seals. It is noted that the pocket damper seal is more suitable for fitting as a drop-in-replacement for conventional labyrinth seals.
- The pocket damper seal has negative direct stiffness, which resulted in reducing the rotor critical speed in tests. Typically, a long labyrinth seal provides negative stiffness as well. Therefore, the critical speed location would not be changed significantly in practice when a long pocket damper seal is used to replace a labyrinth seal. On the other hand, the honeycomb seal has large positive stiffness. It is suggested that to account for the direct stiffness of the honeycomb seal in rotordynamic analyses, whenever a long honeycomb seal is proposed to replace a labyrinth seal. Induced gas swirl at the seal entrance increases the magnitude of the effective stiffness of the test seals. Seal eccentricity results in a decrease in honeycomb seal direct stiffness.
- The existing model of pocket damper seal underpredicts the identified effective damping coefficients of the pocket damper seal consistently in the test pressure range. For the honeycomb seal, the program predicts the damping value well at low pressures and underpredicts the identified effective damping coefficients at high pressures. The damping coefficients calculated by the existing programs are more conservative compared to the experimental results for both honeycomb and pocket damper seals.
- The existing model underpredicts the identified stiffness coefficients of the honeycomb seal in the test pressure range. No obvious trend is identified from the comparison of effective stiffness to predictions for the pocket damper seal.
- In the tested pressure range, the existing computer program underpredicts the leakage of pocket damper seals, while the leakage of honeycomb seals is overpredicted by the model.
- The pocket damper seal leaks more than the honeycomb seal due to the diverging clearance configuration of the pocket seal. The pocket seal has been further improved at the university research laboratory since these tests with eight circumferential pockets in damper cavities and slots in the downstream teeth.

- A design case study of pocket damper seals shows that a carefully selected damper seal with an optimized bearing system could enhance the rotor stability considerably. Of course, the subject rotor should be optimized first before the journal bearing and damper seals are considered further.

REFERENCES

- Armstrong, J. and Perricone, F., 1996, "Turbine Instability Solution-Honeycomb Seals," *Proceedings of the Twenty-Fifth Turbomachinery Symposium*, Turbomachinery Laboratory, Texas A&M University, College Station, Texas, pp. 47-56.
- Childs, D. W., 1993, *Turbomachinery Rotordynamics*, New York, New York: John Wiley & Sons, pp. 290-354.
- Childs, D. W., Elrod, D., and Hals, K., 1989, "Annular Honeycomb Seals: Test Results for Leakage and Rotordynamic Coefficients; Comparisons to Labyrinth and Smooth Configurations," *ASME Journal of Tribology*, 111, pp. 293-301.
- Kleynhans, G. F. and Childs, D. W., 1997, "The Acoustic Influence of Cell Depth on the Rotordynamic Characteristics of Smooth-Rotor/Honeycomb-Stator Annular Gas Seals," *ASME Journal of Engineering for Gas Turbines and Power*, 119, pp. 949-957.
- Li, J., Ransom, D., San Andrés, L., and Vance, J. M., 1999, "Comparison of Predictions with Test Results for Rotordynamic Coefficients of a Four-Pocket Gas Damper Seal," *ASME Journal of Tribology*, 121, (2), pp. 363-369.
- Memmott, E. A., 1999, "Stability Analysis and Testing of a Train of Centrifugal Compressors for High Pressure Gas Injection," *ASME Journal of Engineering for Gas Turbines and Power*, 121, pp. 509- 514.
- Richards, R. L., Vance, J. M., and Zeidan, F. Y., 1995, "Using a Damper Seal to Eliminate Subsynchronous Vibrations in Three Back-to-Back Compressors," *Proceedings of the Twenty-Fourth Turbomachinery Symposium*, Turbomachinery Laboratory, Texas A&M University, College Station, Texas, pp. 59-71.
- Vance, J. M. and Schultz, R. R., 1993, "A New Damper Seal for Turbomachinery," *Proceedings of the Fourteenth Vibration and Noise Conference*, Albuquerque, New Mexico, ASME DE-Vol. 60, pp. 139-148.
- Zeidan, F. Y., Perez, R. X., and Stephenson, E. M., 1993, "The Use of Honeycomb Seals in Stabilizing Two Centrifugal Compressors," *Proceedings of the Twenty-Second Turbomachinery Symposium*, Turbomachinery Laboratory, Texas A&M University, College Station, Texas, pp. 3-15.

ACKNOWLEDGEMENT

The authors are indebted to the Elliott Company for permission to publish this paper, and to the many individuals within the company whose support and assistance made this paper possible.